Solution Structural Studies of Chromatin Fibers†

Keun Su Lee, Marshal Mandelkern, and Donald M. Crothers*

ABSTRACT: We report solution structural studies on 9–16-kilobase (kb) fragments of the 30-nm chromatin fiber isolated from calf thymus nuclei. Samples were stabilized by dimethylsuberimidate cross-linking in 100 mM salt concentration to ensure retention of a compact conformation. Electron microscopy, sedimentation diffusion, light scattering, and gel electrophoresis were used to characterize materials which were fractionated by size by utilizing sucrose gradient sedimentation. Measurements reported include the translational frictional coefficient as determined by quasielastic light scattering and the rotational frictional coefficient as deduced from transient electric dichroism. These frictional properties were combined to yield 33 ± 3 nm for the diameter of the fiber and a length of 1.5 ± 0.1 nm per nucleosome. Assuming a superhelix pitch of 11 nm, we calculate 7.5 ± 0.5 nucleosomes per superhelical turn. The 30-nm fiber was found to reach saturation of electric field orientation at about 10–13 kV/cm and to lack a detectable permanent dipole moment, implying no polarity of the fiber. The limiting reduced dichroism ρ was found to be +0.06, intermediate between the values expected if the nucleosomal disk diameters were parallel (ρ expected = $-^3/_8$) or perpendicular (ρ expected = $+^3/_4$) to the fiber axis. This result implies an average angle of 51° between the fiber axis and the local DNA (nucleosomal) superhelix axis and rules out many of the simple models which have been proposed for the detailed structure of the 30-nm fiber.

Electron microscopy has revealed the presence of fibers roughly 25–30 nm in diameter in chromatin found within eukaryotic cell nuclei (Davies, 1968; Everid et al., 1970; Ris, 1973; Zirkin & Wolfe, 1972; Olins & Olins, 1979; Thoma et al., 1979). These fibers have been interpreted either as helically organized repeating nucleosomal units (Finch & Klug, 1976; Carlson & Olins, 1976; Carpenter et al., 1976; Olins, 1977, 1978) or alternatively as repeating clusters of nucleosomes, or "superbeads" (Renz et al., 1978). Histone H1 is required for condensation of multinucleosomes into the 30-nm fiber (Finch & Klug, 1976; Renz et al., 1977; Thoma et al., 1979). Solution studies of the fiber have been hampered by its fragility: exposure to salt concentration below about 50 mM causes morphological and physical changes (Thoma et al., 1979; Campbell et al., 1978) whereas salt concentrations above about 150 mM cause chromatin precipitation and removal of histone H1. Enzymatic and mechanical (shear) degradation are also serious problems in working with chromatin fibers.

Our approach to study of the solution properties of these fibers utilizes material stabilized by protein–protein cross-linking, carried out in 100 mM salt to assure retention of a compact structure. We had earlier observed that dimethylsuberimidate-cross-linked nucleosomes were identical with control nucleosomes in linear dichroism and rotational correlation time (Wu et al., 1979), implying no change in DNA winding or nucleosome size as a consequence of cross-linking. Hence we reasoned that chromatin fibers could be cross-linked in high salt and subsequently studied in the low salt buffers necessary for electrooptical measurements. Retention of conformation in the cross-linked samples is further assured by inclusion of a preparatory step which selects for material whose *s* value is unchanged when it is exposed to low salt concentration under conditions which cause the *s* value of un-cross-linked chromatin to decrease sharply.

In addition to standard measurement of particle molecular weight and CD spectra, we have determined both the rotational and translational frictional coefficients of stabilized chromatin fibers. The data are analyzed by using hydrodynamic equations for cylinders, yielding nearly constant diameter and rise per nucleosome for a set of fibers of varying length. A similar analysis of cylinder length and diameter by electric birefringence and quasielastic light scattering has been reported for filamentous viruses by Newman et al. (1977) and Chen et al. (1980), who found good agreement with dimensions determined by electron microscopy.

We have also measured the linear dichroism of the chromatin fiber by orienting the sample in an electric field. In contrast to DNA (Ding et al., 1972; Hogan et al., 1978), nucleosomes (Crothers et al., 1978), and chromatin fibers cross-linked in lower salt (K. S. Lee and D. M. Crothers, unpublished results), all of which show negative dichroism, the dichroism of stabilized compact chromatin fibers isolated from calf thymus nuclei is positive. We use the results to estimate the angle formed between the nucleosomal disks and the superhelical axis of the fiber.

Materials and Methods

Preparation of Nuclei and Solubilized Chromatin. Calf thymus nuclei were prepared by modification of the method of Blobel & Potter (1966). A 50-g sample of frozen thymus was minced and homogenized in 200 mL of solution A (0.3 M sucrose, 50 mM triethanolamine, 25 mM KCl, 5 mM $MgCl_2$, and 1 mM $PhCH_2SO_2F$, pH 6.8 at 4 °C) by using a Waring blender at 40 V for 5 min. After filtration through cheesecloth, nuclei were pelleted at 800*g* for 10 min and washed several times with solution A and then with solution B (0.3 M sucrose, 50 mM triethanolamine, 25 mM KCl, 4 mM $MgCl_2$, 1 mM $CaCl_2$, and 1 mM $PhCH_2SO_2F$ (PMSF), pH 7.8, at 4 °C). Nuclei were resuspended in solution B to a concentration of 100 OD_{260} and digested with 1–10 units of micrococcal nuclease mL^{-1} at 4 °C for 0.5 h. The digestion was stopped by the addition of EDTA to a final concentration of 5 mM. In order to get a higher yield of large fragments of chromatin, sometimes nuclei were incubated in solution B at 4 °C for 2–3 h without exogenous micrococcal nuclease. Nuclei were pelleted and washed once with solution A, then lysed with equal volumes of lysis buffer (0.2 mM EDTA,

† From the Department of Chemistry, Yale University, New Haven, Connecticut 06520. *Received October 3, 1980.* Supported by Grant GM 21966 from the National Institutes of Health. This paper is dedicated to the late H. J. Li.

0006-2960/81/0420-1438$01.25/0

titrated to pH 7.0 at 4 °C with Tris) for 0.5 h. Nuclear debris was removed by centrifugation at 10000*g* for 15 min, the chromatin supernatant was loaded on a 10–30% sucrose gradient in cross-linking buffer, and appropriate fractions of polynucleosomes were collected and dialyzed against the cross-linking buffer. Sometimes this preliminary fractionation of chromatin was omitted, and the total soluble chromatin was dialyzed directly against the cross-linking buffer.

Reaction with Dimethylsuberimidate (DMS). Chromatin in cross-linking buffer (10 mM Hepes, 0.1 mM EDTA, 1 mM PMSF, and 100 mM NaCl, pH 8.0) was adjusted to A_{260} = 10 and placed inside a dialysis bag which was clamped at one end with a closure for easy opening and closing.

Dimethylsuberimidate was dissolved rapidly into a desired volume of the cross-linking buffer to a final concentration of 20 mg mL^{-1} (the pH of the cross-linking buffer had been adjusted before adding DMS in order to give the correct pH after DMS addition). DMS solution (0.1 volume) was then immediately added to the chromatin solution inside the dialysis bag, which was maintained in continuous dialysis against the cross-linking buffer. After a 30-min waiting period, another portion of freshly dissolved DMS solution was added, and the same steps were repeated until extensive cross-linking was achieved. Then the chromatin solution was dialyzed against 0.1 mM Tris and 0.1 mM EDTA, pH 7.8.

Fractionation of Chromatin. The solution of cross-linked chromatin was concentrated to 20 OD_{260} mL^{-1} in 0.1 mM Tris and 0.1 mM EDTA, pH 7.8, and loaded on a 10–30% sucrose gradient in the same buffer. Centrifugation utilized a SW27 rotor at 25 000 rpm for 4–7 h depending on the size range of polynucleosomes being fractionated. After centrifugation, fractions were collected and dialyzed against either 0.1 mM Tris and 0.1 mM EDTA, pH 7.8, or 0.1 mM Tris and 0.1 mM $MgCl_2$, pH 7.8.

Gel Electrophoresis. DNA was extracted from chromatin by incubation at 37 °C with 100 μg mL^{-1} of proteinase K in 1 M NaCl for 3 h, followed by precipitation with 2 volumes of 95% ethanol. Agarose gel electrophoresis of DNA was performed as described by McDonnell et al. (1977). Electrophoresis buffer contained 50 mM phosphate and 2 mM EDTA, pH 7.0. In some cases, 0.1% $NaDodSO_4$ was added to both sample buffer and running buffer. Gels were run on a horizontal apparatus at 3 V cm^{-1} and stained with 1 μg mL^{-1} ethidium bromide.

The 5% sodium dodecyl sulfate slab gels were run according to Weber & Osborn (1969). Polynucleosomes were treated with sample buffer containing 1% $NaDodSO_4$ and 100–500 μg was loaded on each slot. In some cases polynucleosomes were lyophilized before resuspending in the sample buffer.

Electron Microscopy. Electron micrographs were taken with a Philips 300 electron microscope at 60 kV. Size calibration was based on examination of diffraction grating replicas. The 400-mesh parlodion-coated grids were coated with carbon and floated on ethanol for 1 h, followed by air-drying.

Polynucleosomes fixed with DMS were diluted at room temperature with 0.1 mM Tris and 0.1 mM EDTA (or $MgCl_2$), pH 7.8, to an A_{260} of 0.03–0.08 and then absorbed by floating the grid for 1 min. The grids were stained with 2% uranyl acetate in water for 30 s, rinsed with water for 1 min, dehydrated for 2–3 s in ethanol, and blotted dry on filter paper. For contrast enhancement, the grids were rotary shadowed at an angle of 8° with Pt–Pd.

Circular Dichroism. Circular dichroism measurements were obtained at room temperature on a Cary 60 with CD attachment. Concentrations of DNA nucleotide residues in chromatin were determined by absorption at 260 nm using ϵ_{260} = 6600 cm^{-1} (mol of phosphate)$^{-1}$. Samples used were (1.0–2.0) × 10^{-4} M phosphate in 0.1 mM Tris and 0.1 mM $MgCl_2$, pH 7.8.

Analytical Ultracentrifugation. Ultracentrifugation studies were performed on a Spinco Model E analytical ultracentrifuge with a photoelectric scanning system and a RTIC temperature control. Scans were taken at 266 nm and 20 °C. A value for the partial specific volume ($\bar{v}$) of 0.66 mL/g (Olins et al., 1976) was employed in calculating molecular weights.

Light-Scattering Intensity Measurements. Scattered light intensity was measured as a function of DNA concentration and scattering angle. The instrument is a Malvern photometer with an argon laser at λ 488.0 nm. The system was calibrated following the methods of Eisenberg & Tomkins (1968). $\delta n/\delta c$ was measured by using a Brice-Phoenix differential refractometer.

Dynamic Light Scattering. The fixed polynucleosomes were clarified by Millipore filtration and used at A_{260} = 0.1–2. The incident light was from an argon laser, λ 488.0 nm. The autocorrelation function was calculated by a Malvern K7025 correlator and fit by a least-squares routine to a single exponential curve. The decay constant is related to the diffusion coefficient by $1/\tau^{(i)} = 2q^2D^{(i)}$, where q, the scattering vector, has magnitude $(4\pi\eta/\lambda) \sin(\theta/2)$. The scattering angle θ was 90° and temperature was 20.0 °C, unless specified otherwise.

Electric Dichroism. Electric dichroism was measured on a device originally designed for temperature-jump kinetic studies and modified by placing a prism polarizer in the incident beam just in front of the temperature jump cell (Hogan et al., 1978). The prism was in a mount that could be rotated to any desired angle. The temperature jump cell had an optical path length of 0.7 cm and an electrode separation of 1.18 cm.

Samples (1.3 mL) containing approximately 0.4–0.8 A_{260} were subjected to field strengths ranging 1–30 kV/cm. Several successive traces were averaged for each measurement of the reduced dichroism or rotational correlation time.

Results

Preparation of Cross-Linked Fibers Whose s Value Is Independent of Salt Concentration. Polynucleosomes fractionated by sucrose gradient centrifugation were subjected to DMS cross-linking as described under Materials and Methods. The crucial factor in this procedure is to keep the DMS additions small enough so that the ionic strength and pH change contributed by the imidate salt and its hydrolysis do not result in histone H1 dissociation. This we accomplished by repeated small additions of DMS to the reaction mixture, which was kept in dialysis contact with buffer to prevent pH drift. Under these conditions, roughly seven additions of DMS were sufficient to cross-link all the histones to the extent that no protein could be observed to enter a sodium dodecyl sulfate–5% acrylamide gel (Figure 1a). In contrast, when 2.5 times larger additions of DMS were made, an octamer band persisted in the gel profile (Figure 1b), accompanied by the presence of slowly sedimenting material [data not shown; see Lee (1980)]. This failure of complete cross-linking in Figure 1b may result from the high ionic concentration or large pH drift which follow large additions of DMS.

Retention of frictional properties after cross-linking and resistance of the cross-linked structure to conformational change can both be assayed by comparing the sedimentation profiles, in cross-linking buffer (100 mM salt) and in low salt buffer, of cross-linked and un-cross-linked samples. Figure 2 summarizes the results. The fixed and unfixed samples sedimented identically in cross-linking buffer (dotted line), and

Table I: Molecular Weights of Chromatin Fibers Cross-linked at 100 mM Salt and Measured at 0.1 mM Tris and 0.1 mM $MgCl_2$, pH 7.8

sample	$s_{20,w}$ (S)	$D_{20}^{(t)} \times 10^8$ ($cm^2\ s^{-1}$)	DNA size,[a] kbp	M_r[b] (10^{-6})	M_r[c] (10^{-6})	M_r[d] (10^{-6})	no. of nucleosomes[e]
1	177 ± 5	5.98 ± 0.05	16 ± 2	21 ± 2	21.9 ± 0.5	21 ± 1	82 ± 4
2	145 ± 5	7.00 ± 0.05	12 ± 2	16 ± 2	15.3 ± 0.5	15 ± 1	61 ± 3
3	125 ± 5	7.83 ± 0.05	9 ± 1.5	12 ± 1.5	11.8 ± 0.5		46 ± 3

[a] The uncertainties indicate the breadth of the DNA bands on 0.5% agarose gel. [b] Calculated from DNA size and protein:DNA = 1:1. [c] Calculated from $M = SNkT/[D^{(t)}(1 - \bar{v}\rho)]$ with $\bar{v} = 0.66$ and $\rho = 1.00$ (Olins et al., 1976). [d] Calculated from Zimm plot by using $\delta n/\delta c = 250 \times 10^{-6}$ mL mg^{-1}. [e] Number of nucleosomes was calculated from DNA size and 195 bp/nucleosome for calf thymus chromatin (Steinmetz et al., 1978).

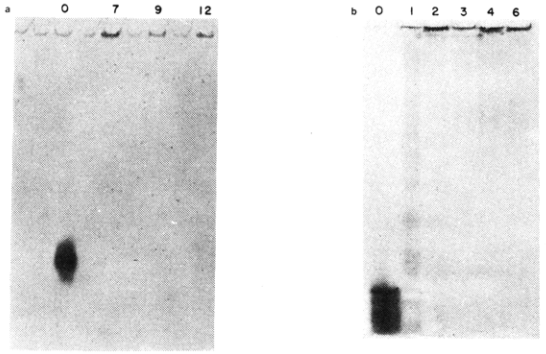

FIGURE 1: (a, left) 5% $NaDodSO_4$–polyacrylamide gel for polynucleosomes fixed as described under Materials and Methods. The number of DMS addition is indicated for each slot. The cross-linking buffer was 10 mM Hepes, 0.1 mM EDTA, 100 mM NaCl, and 1 mM PMSF, pH 8.0. (b, right) 5% $NaDodSO_4$–polyacrylamide gel of histones cross-linked with 2.5 times larger additions of DMS than in (a). Polynucleosomes (10 OD_{260}) were fixed with DMS (0.25 volume of 20 mg mL^{-1}) at 10 mM HEPES, 0.1 mM EDTA, and 1.0 mM PMSF, pH 8.0. The number of DMS additions is shown for each slot.

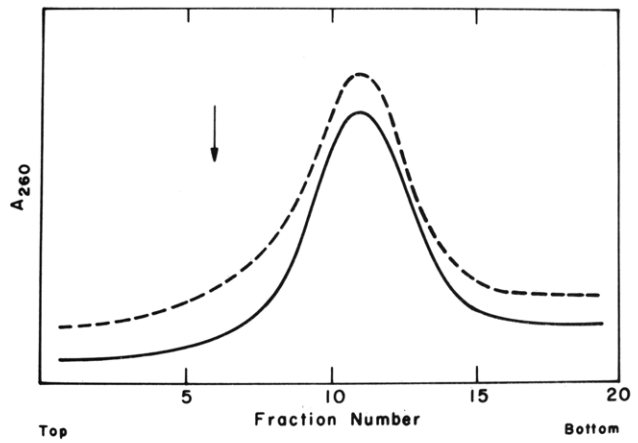

FIGURE 2: Sucrose gradient profile for polynucleosomes cross-linked at 10 mM Hepes, 0.1 mM EDTA, 100 mM NaCl, and 1 mM PMSF, pH 8.0 (solid line). The gradient was 10–30% sucrose in 0.1 mM Tris and 0.1 mM EDTA, pH 7.8. Centrifugration utilized a SW27 rotor at 25 000 rpm for 5 h. The dotted line shows the profile for fixed and unfixed samples sedimented in cross-linking buffer. The arrow indicates the peak position of unfixed sample in 0.1 mM Tris and 0.1 mM EDTA, pH 7.8.

the mean s value of the fixed sample was unaltered in low salt buffer (solid line). When an unfixed sample was run in low salt buffer, its sedimentation maximum was at the position indicated by the arrow. Hence we conclude that, as found for nucleosomes (Wu et al., 1979), cross-linking prevents the unfolding which is characteristic of unfixed chromatin upon exposure to low salt buffer.

Investigation of Electrostatic Effects on the Diffusion Coefficient. The electric dichroism method requires low salt concentrations in order to reduce solution conductivity, especially if the rotational correlation time is long, thus necessitating an electric field of long duration. An important question is the effect of lowered salt concentration on the transport coefficients. Our preparative sucrose gradient runs indicated minimal effect of lowered salt concentration on s value, but the sedimentation coefficient (and rotational relaxation time) cannot presently be measured with the accuracy with which we can determine the diffusion constant of large chromatin fragments (1%) by quasielastic light scattering. Hence we examined the salt dependence of the translational correlation time $\tau^{(t)}$ at different salt concentrations. Figure 3 shows characteristic results. At a concentration of 0.1 A_{260} there is no detectable dependence of $\tau^{(t)}$ on salt concentration from 10 mM down to 0.5 mM ionic strength. At higher concentration (0.4 A_{260}) there is a slight (5%) increase of $\tau^{(t)}$ at 0.5 mM above the value at 10 mM ionic strength. Hence we conclude that there is no significant effect of salt concentration on transport coefficients extrapolated to zero polymer concentration. However, the virial (or polymer concentration dependent) effects can change appreciably as the ionic strength is varied.

Determination of Fiber Molecular Weights. We measured the molecular mass of fixed chromatin fibers by light scattering, sedimentation diffusion, and agarose gel electrophoresis of DNA samples extracted from the particles, with good agreement between all three methods.

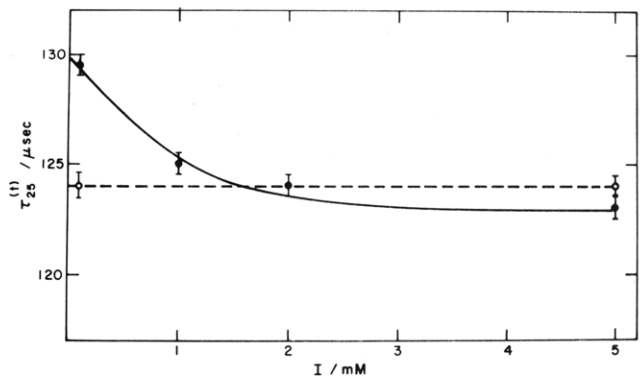

FIGURE 3: Effect of polynucleosome concentration on $\tau^{(t)}$. $\tau^{(t)}$ was measured as a function of ionic strength at $OD_{260} = 0.38$ (●) or at $OD_{260} = 0.12$ (○). The lowest ionic strength corresponds to 0.1 mM Tris and 0.1 mM $MgCl_2$, pH 7.8, and NaCl was added to raise the ionic strength. The temperature was 25 °C.

Figure 4 shows a Zimm plot of light scattering data from a typical polynucleosome fraction, from which the weight-average molecular weight was calculated in the usual way. Agarose gels (Figure 5) of DNA extracted from the polynucleosomes also provide a molecular weight estimate, using the assumption of a 1:1 protein to DNA weight ratio in the fiber. In addition, we measured the diffusion constant and sedimentation coefficient for each sample, and calculated the molecular weight. The results of these experiments are summarized in Table I, from which it can be seen that all three methods used agree within experimental error.

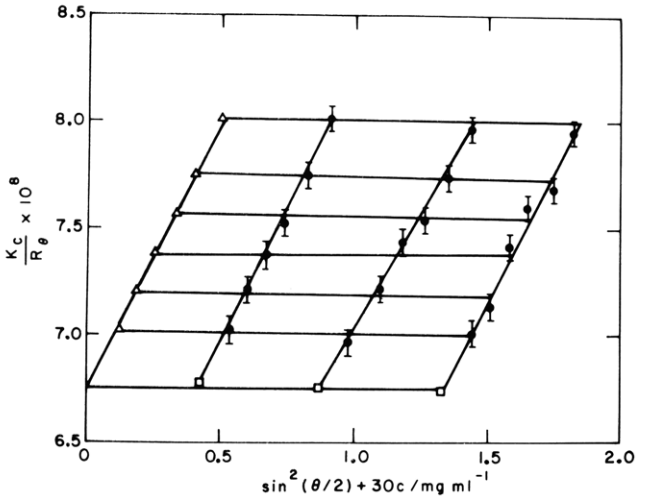

FIGURE 4: Zimm plot showing light scattering from a sample containing 60 nucleosomes per polynucleosome. Measurements were done at 20.0 °C in 0.1 mM Tris and 0.1 mM $MgCl_2$, pH 7.8.

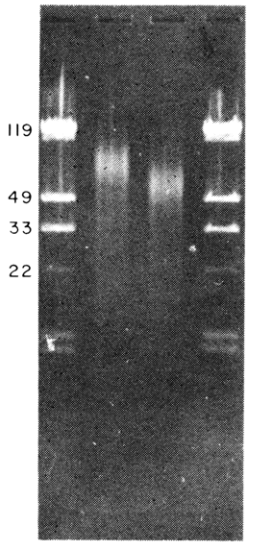

FIGURE 5: Sizing of polynucleosome fractions on 0.5% agarose gel. Calibration was done with *Hin*dIII digest of λ DNA and the numbers on the left denote number of nucleosomes. Sample lanes contain 16 and 12 kb DNA, respectively.

Circular Dichroism of the Stabilized Fiber. Cross-linking with DMS does not introduce new chiral centers in chromatin, nor does it affect the UV spectrum. Hence it is reasonable to examine the CD spectrum of the cross-linked fiber. Figure 6 shows the results obtained for chromatin cross-linked at 100 mM salt concentration. An ellipticity maximum occurs at 283 nm, of amplitude $[\theta]_{283} = 2500 \pm 400$ deg cm^2/dmol PO_4, with a shoulder at 274 nm, $[\theta]_{274} = 2100 \pm 400$ deg cm^2/dmol PO_4. Crossover to negative values occurs at 265 cm. These values are in good agreement with the results obtained by de Murcia et al. (1978) ($[\theta]_{283} \approx 2000$ deg cm^2/dmol PO_4) who confirmed the compact state of their chromatin by electron microscopy. Higher ellipticities in lower ionic strength media ($[\theta]_{283} \approx 4000$ deg cm^2/dmol PO_4) have been measured by Fulmer & Fasman (1979) and others. We believe that the higher ellipticity values result from unfolding of chromatin superstructure, consistent with the observation by Cowman & Fasman (1978) of $[\theta]_{283} \approx 4000$ deg nm^2/dmol PO_4 for 200 bp mononucleosomes. Hence it appears that the higher order folding of chromatin contributes to the CD spectrum in a significant way.

Electron Microscopy of Cross-Linked Chromatin. We verified the fiberlike character of DMS cross-linked chromatin

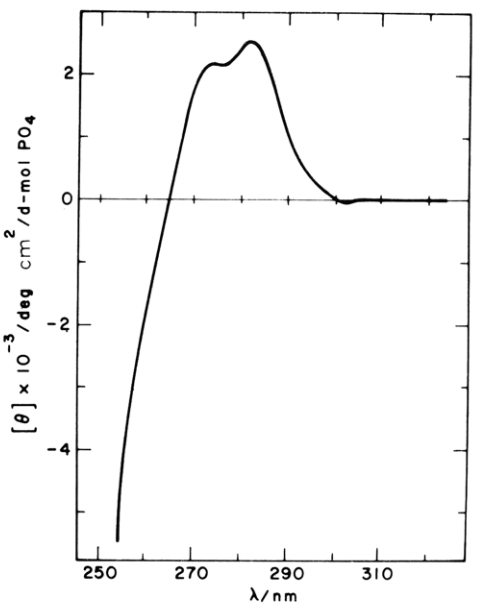

FIGURE 6: CD spectrum of polynucleosomes cross-linked at 100 mM salt, recorded at 20 °C, in 0.1 mM Tris and 0.1 mM $MgCl_2$, pH 7.8.

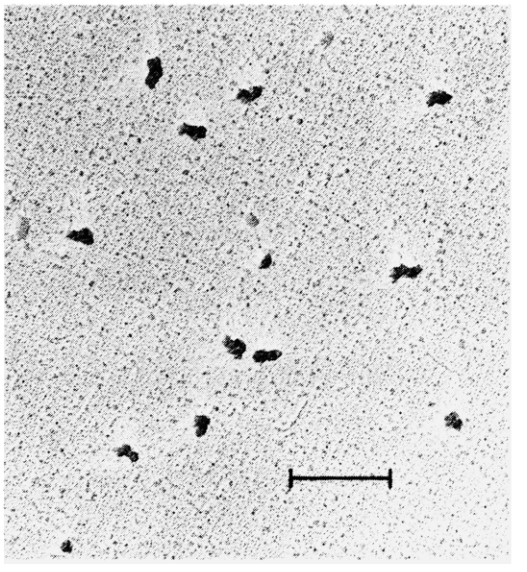

FIGURE 7: Electron micrograph of polynucleosomes fixed with DMS at 100 mM salt. The polynucleosomes in this sample contain an average of 60 nucleosomes. The spreading buffer was 0.1 mM Tris, 0.1 mM $MgCl_2$, pH 7.8, and the bar represents 3000 Å.

fragments by electron microscopic observations. Samples cross-linked in 100 mM salt were dialyzed either into 0.1 mM Tris and 0.1 mM $MgCl_2$ (pH 7.5), or into 0.1 mM Tris and 0.1 mM EDTA (pH 7.5) and spread on grids in the same buffer. A typical field is shown in Figure 7. The chromatin fibers appeared compact, with a fairly uniform diameter of about 300–350 Å. Axial ratios of the particles are consistent, within experimental error (±20%), with the values obtained from hydrodynamic measurements described below. As documented extensively in earlier work (Griffith & Christiansen, 1978; Thoma et al., 1980), chromatin fixed at lower ionic strengths is less compact. Our observations on low-salt fixed material are consistent with this finding and indicate substantial differences in hydrodynamic and dichroism properties from high-salt fixed samples (K. S. Lee and D. M. Crothers, unpublished results).

Electric Dichroism of Stabilized Chromatin Fibers. Previous electric dichroism studies of chromatin utilized samples

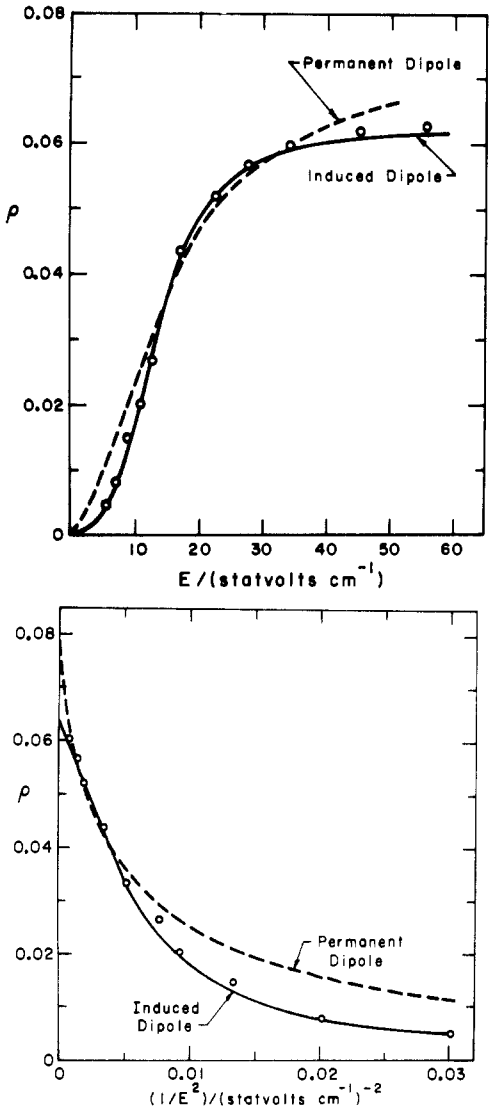

FIGURE 8: (a, upper) Field dependence of electric dichroism of polynucleosomes fixed at 100 mM salt. The adjustable parameters giving best fit to the induced dipole model were $\Delta\alpha = 1.5 \times 10^{-15}$ cm^3 and $\rho = 0.063$, and for the permanent moment model $\mu = 10\,800$ D and $\rho = 0.084$. (O) Experimentally measured points for 62 nucleosome polynucleosomes in 0.1 mM Tris and 0.1 mM $MgCl_2$, pH 7.8; temperature 12 °C. (b, lower) Extrapolation to infinite field by using a plot of ρ versus $1/E^2$ for the data in (a).

in the gel state (Houssier & Fredericq, 1966) or sheared chromatin solutions at low ionic strength (Rill & van Holde, 1974; Houssier et al., 1977). Recently Marion & Roux (1978) applied electric birefringence to the study of small oligomers of nucleosomes. The results showed a sharp transition in the electrooptical properties when the number of nucleosomes is greater than six: the initial negative birefringence became positive, and the rotational relaxation time increased sharply.

Our results show positive dichroism for the compact chromatin fiber, in contrast to the negative dichroism of DNA and nucleosomes. Determination of the limiting dichroism at perfect orientation requires an extrapolation to inifinite field, as shown in Figure 8a,b. Figure 8b shows that the dichroism at high field is a linear function of $1/E^2$, as expected for an induced dipole moment (O'Konski et al., 1959). Figure 8a shows the observed field dependence of the dichroism compared with prediction based on permanent dipole and induced dipole mechanisms, using the equations given by O'Konski et al. (1959). Only the induced moment function fits the experimental points adequately. The limiting dichroism, 0.063 ± 0.005, was found to be independent of polynucleosome length in the range studied (40–100 nucleosomes).

Table II: Translational and Rotational Correlation Times of Polynucleosomal Samples[a]

DNA size (kb)	no. of nucleosomes	$\tau^{(t)}$ (μs)[b]	$\tau^{(r)}$ (μs)[c]
9	46	105	33
12	61	117	52
17	82	137	93

[a] Corrected to 20 °C; measured in 0.1 mM $MgCl_2$ and 0.1 mM Tris, pH 8. [b] Measured at 20 °C and scattering angle $\theta = 90°$ and corrected to zero polynucleosome concentration. [c] Measured at 12 °C and corrected to 20 °C.

The difference in polarizability along the long and short axes was found to be $\Delta\alpha = 1.5 \times 10^{-15}$ cm^3 for a sample containing 60 nucleosomes, in 0.1 mM Tris and 0.1 mM Mg Cl_2, pH 7.8. We found $\Delta\alpha$ to be proportional to polynucleosome length and also proportional to the reciprocal square root of conductivity of the measurement buffer, as will be reported in detail later (K. S. Lee and D. M. Crothers, to be published).

The dichroism ρ was independent of the ionic strength of the measurement buffer. However, samples imperfectly cross-linked, or cross-linked at NaCl concentrations below 80–100 mM, gave pronounced differences in the dichroism behavior, including negative (–0.1 to –0.2) rather than positive dichroism. In addition, instead of saturating at 10–13 kV/cm (33–40 statV/cm) as seen for the positive dichroism in Figure 8a, the negative dichroism for samples cross-linked at lower salt showed no saturation even up to 30–35 kV/cm. As discussed elsewhere in more detail (K. S. Lee and D. M. Crothers, unpublished results), we believe that the negative dichroism of less compact fibers arises from a field-induced internal deformation or segmental orientation in these more flexible polynucleosomes.

Determination of the Rotational Diffusion Constant. The dichroism of molecules containing a purely induced dipole moment is expected to rise to its steady-state value, $\rho(ss)$, according to (Tinoco, 1955)

$$\rho(t) = \rho(ss)[1 - \exp(-6D^{(r)}t)]$$

in which $D^{(r)}$ is the rotational diffusion constant for reorientation of the long axis. (We assume that the molecule is optically isotropic about its cylindrical axis.) Hence the relaxation time for rotational motion is $\tau^{(r)} = 1/6D^{(r)}$.

We verified that $\rho(t)$ rises with a single exponential, within the noise of the data. (The small limiting dichroism, $\rho_\infty = 0.063$, produces noisy signals, signal-to-noise ratio ~5–10, about 10–20 times smaller than for DNA.) We also confirmed that $\tau^{(r)}$ varies linearly with solution viscosity as affected by addition of sucrose; see Lee (1980) for details. This result is expected if frictional resistance to rotation limits the dichroism rise time.

A distinct problem in the determination of $\tau^{(r)}$ was the field dependence observed. Because of the small signal, we could not measure $\tau^{(r)}$ below about 17% orientation and hence were forced to extrapolate $\tau^{(r)}$ to degree of orientation $\Phi = \rho_E/\rho_\infty = 0$. These results are shown in Figure 9, revealing a substantial correction for the sample containing 16 kb of DNA, with smaller field dependencies for the lower molecular weight sample. Within the error limits of the measurement we could not detect a concentration dependence of $\tau^{(r)}$. Table II summarizes the rotational and translational relaxation times of the three main samples used in this study.

The data in Table II show that $\tau^{(r)}$ and $\tau^{(t)}$ are comparable, raising the question of the possible contribution of rotational motion to the light scattering fluctuations used to determine

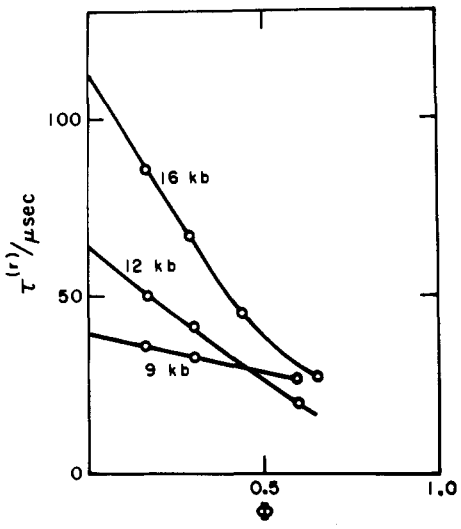

FIGURE 9: Field dependence of the orientation time of polynucleosomes with different sizes. $\tau^{(r)}$ measured at 12 °C is plotted against the orientation function Φ and extrapolated to zero. The size of polynucleosomal DNA is indicated for each sample.

$\tau^{(t)}$. We verified that $1/\tau^{(t)}$ was linear in q^2, where $q = (4\pi\eta/\lambda) \sin(\theta/2)$, as should be the case for purely translational motion. We surmise that the small optical anisotropy of the particle, as reflected in its small dichroism, may cause rotational contributions to scattering fluctuations to be negligible.

Discussion

Interpretation of the Hydrodynamic Parameters. Data on the translational and rotational motion of chromatin fibers can be combined with the assumption that the fibers behave hydrodynamically as cylinders to yield the length L and diameter d or axial ratio $p = L/d$ of each particle. This analysis requires in addition some results from hydrodynamic theory. There are three readily interchangeable ways to characterize the rate of translational or rotational motion: in terms of the diffusion constants $D^{(t)}$ and $D^{(r)}$, the corresponding frictional coefficients $f^{(t)}$ and $f^{(r)}$, with

$$D = kT/f$$

in each case, or the relaxation times $\tau^{(t)}$ and $\tau^{(r)}$:

$$\tau^{(t)} = 1/(2q^2D^{(t)})$$

$$\tau^{(r)} = 1/(6D^{(r)}) \text{ (induced dipole)}$$

In the first of these equations, q depends on refractive index η, wavelength λ, and scattering angle θ according to

$$q = (4\pi\eta/\lambda) \sin(\theta/2)$$

The second equation is modified to $\tau^{(r)} = 1/2D^{(r)}$ when the particle orients with a permanent dipole moment along the electric field, and the orientation rise time is measured.

The standard form for expressing the rotational and translational frictional coefficients (Broersma, 1960; Tirado & Garcia de la Torre, 1979) is

$$f^{(t)} = 3\pi\eta L/(\ln p + \gamma^{(t)})$$

$$f^{(r)} = \pi\eta L/[3(\ln 2p - \gamma^{(r)})]$$

in which η is the solvent viscosity, and the γ are correction factors which account for end effects. The factor $\gamma^{(t)}$ has been extensively tabulated by Tirado & Garcia de la Torre (1979), including values for cylinders of short axial ratio, but there appears to be no calculation of comparable accuracy for rotation of short cylinders. Hence we measured the frictional coefficient of macroscopic cylinders with $p \geq 1$ (M. Mandelkern and D. M. Crothers, unpublished results) and found that the data could be fit by

$$\gamma^{(r)} = 0.0197p^3 - 0.2289p^2 + 0.9706p - 0.2463 \quad (1 \leq p \leq 5)$$

This expression was used in the subsequent analysis.

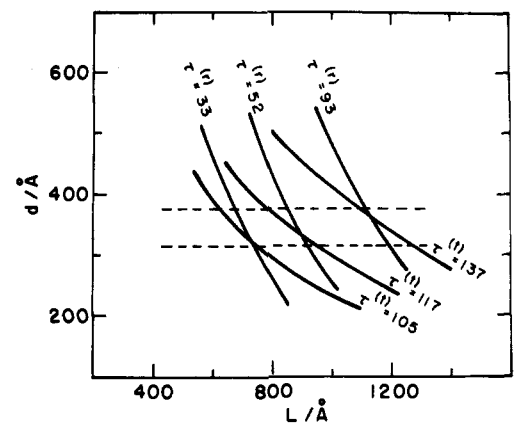

FIGURE 10: Plots of constant (observed) values of $\tau^{(r)}$ and $\tau^{(t)}$ for three different polynucleosomal samples, at varying L and d. From each intersection we obtain d = 325 Å, L = 725 Å for 46-mer, d = 330 Å, L = 900 Å for 61-mer, and d = 360 Å, L = 1125 Å for 82-mer.

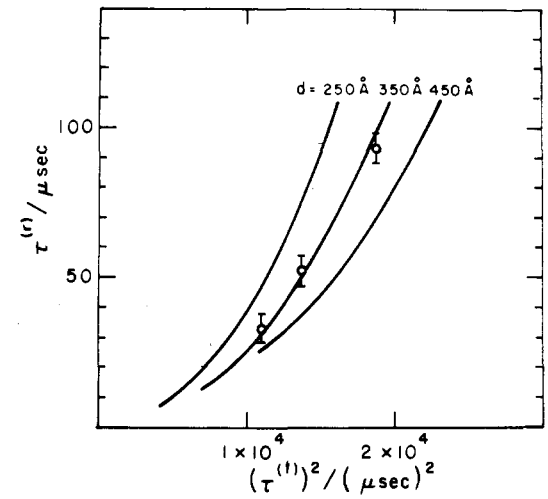

FIGURE 11: Plots of experimental (O) values of $\tau^{(r)}$ as a function of $(\tau^{(t)})^2$, compared with theoretical curves of three different diameters d = 250, 350, and 450 Å, and varying length.

Given two measured parameters ($f^{(t)}$ and $f^{(r)}$), two unknowns (L and p or d), and two nonlinear equations, it is possible to devise graphical methods to solve the simultaneous equations [see Newman et al. (1977) and Chen et al. (1980)]. Two examples are shown in Figures 10 and 11. In Figure 10, for varying L we found the diameter d which would produce the observed values of $\tau^{(t)}$ or $\tau^{(r)}$. Intersection of the two constant τ curves for a given particle implies L and d values which satisfy both $\tau^{(r)}$ and $\tau^{(t)}$. Examination of the figure also shows that, of the two constant τ curves, the curve for constant $\tau^{(r)}$ is more sensitive to a given fractional change in τ. Hence accuracy in $\tau^{(t)}$ is more important than in $\tau^{(r)}$, a condition which our experiments fulfill.

Figure 11 shows an alternative approach to analysis of the data, in which $\tau^{(r)}$ is plotted as a function of $[\tau^{(t)}]^2$ for the series of particles. ($\tau^{(t)}$ is squared in order to make the plots roughly

Table III: Diameter and Length of Polynucleosomal Fibers[a]

no. of nucleosomes	d (Å)	L (Å)	rise/nucleosome (Å)
46	325	725	15.8
61	330	900	14.8
82	360	1125	13.7

[a] Determined from the intersection points in Figure 10. Chromatin fixed in 100 mM salt; dimensions measured in 0.1 mM $MgCl_2$ and 0.1 mM Tris, pH 7.8.

linear.) Theoretical curves are calculated in which the particle has constant diameter and varying length, conditions for which $\tau^{(r)}$ and $\tau^{(t)}$ are readily calculated. As seen in Figure 11, the particles fall close to the line with diameter 350 Å, in agreement with the average intersection diameter of about 330–340 Å in Figure 10. Once the diameter is fixed, the length of the particles is readily calculated from either $\tau^{(r)}$ or $\tau^{(t)}$. Table III summarizes the dimensional properties which we determined for the set of stabilized chromatin fibers.

Stiffness of the Polynucleosonal Fiber. The hydrodynamic analysis we have presented is valid only as long as the fiber is short enough to be considered a cylinder, generally smaller than a persistence length. Constancy of measured diameter and rise per residue over the length range examined is a test of the validity of the cylindrical model. The variation of diameter and rise per residue we observe is virtually within the error range of our measurements, but these does seem to be a systematic drift to larger diameter and shorter rise per residue as the fiber length increases. This is the result expected if the fiber has some flexibility in the range studied. In addition, the appearance of the electron micrographs suggests appreciable bending of the $n = 82$ sample, and the large electric field dependence of the orientation time of the $n = 82$ sample also implies appreciable flexibility. As a very rough estimate, we suggest that the persistence length of the compact polynucleosomal fiber may be about 1000 Å.

Interpretation of the Dichroism. The main complication in interpreting the value of the fiber dichroism ($\rho = 0.063 \pm 0.005$) is the unknown path of the linker DNA. We adopt here the simplest possible assumption, which is that the linker DNA continues on the same superhelical path as the core DNA. This results in an integral number of half-turns of DNA about the nucleosomal superhelix axis: 2 turns if 200 bp are wound at 100 bp/turn as we have suggested (Crothers et al., 1978) or 2.5 turns if the winding is at the more standard value of 80 bp/turn (Finch et al., 1977).

The dichroism of a nucleosomal disk with an integral number of half-turns can be expressed by (Crothers et al., 1978)

$$\rho = -\tfrac{3}{8}(3\langle\cos^2\alpha\rangle - 1)(3\cos^2\beta - 1)(1 - 3\cos^2\gamma_1)$$

in which α is the angle between the DNA base transition moments and the DNA helix axis, β is the angle between the DNA helix and the nucleosomal superhelix axis, and γ_1 is the angle between the normal to the plane of the nucleosomal disk and the chromatin fiber axis. Our earlier work on nucleosome dichroism showed that the data were consistent with $\alpha = 90°$, $\beta = 85°$. Using these values and $\rho = 0.063$ we obtain $\gamma_1 = 51°$. Whatever assumption is made about the path of the linker DNA, it is clear that the nucleosomal superhelix axis can be neither parallel nor perpendicular to the fiber axis, and one is forced to consider models in which the disks are angularly placed relative to the fiber axis.

Lack of Polarity of the Fiber. Our results showed no appreciable permanent dipole moment of the polynucleosomal fibers. Since individual disks have a dipole moment of more than 1000 D, the lack of any appreciable resultant moment along the fiber axis means either (a) that the nucleosomal dyad axis is perpendicular to the fiber axis or (b) that nucleosomes alternate in their placement so that their successive components along the fiber axis cancel.

Table IV: Solution Structural Properties of Chromatin Fibers

diameter, d (Å)	330 ± 30
rise per nucleosome, h (Å)	15 ± I
nucleosomes per superhelical turn	7.5 ± 0.5
average angle between nucleosome DNA superhelix axis and fiber axis, γ_1 (deg)	51

Summary of the Results. Our characterization of the polynucleosomal fiber in solution is summarized in Table IV. The number of nucleosomes per superhelical turn was calculated by dividing the estimated superhelix pitch of 110 Å (Finch & Klug, 1976; Suan et al., 1979) by our measured rise per nucleosome. The dimensions which we determined are in good agreement with those determined by other methods, such as neutron scattering (Suan et al., 1979) and electron microscopy (Thoma et al., 1979), reinforcing our confidence in the structural integrity of polynucleosomal fibers fixed by protein–protein cross-linking. In addition, the measured dichroism of +0.06 provides new insight into the organization of DNA in chromatin fibers. The results rule out a number of structural models for the solenoidal fiber, particularly those in which the nucleosomal disks are arranged so that their diameters are either parallel (Worcel & Benyajati, 1977; Thoma et al., 1979) or perpendicular (Suan et al., 1979) to the solenoidal fiber axis. However, more detailed structural information is needed before we can construct an accurate model which accounts for the average 51° angle which we find between the local DNA superhelix axis and the solenoidal fiber axis.

References

Blobel, G., & Potter, V. R. (1966) *Science (Washington, D.C.) 154*, 1662–1665.

Broersma, S. (1960) *J. Chem. Phys. 32*, 1626–1631.

Campbell, A. M., Cotter, R. I., & Pardon, J. F. (1978) *Nucleic Acids Res. 5*, 1571–1580.

Carlson, R. D., & Olins, D. E. (1976) *Nucleic Acids Res. 3*, 89–100.

Carpenter, B. G., Baldwin, J. P., Bradbury, E. M., & Ibel, K. (1976) *Nucleic Acids Res. 3*, 1739–1796.

Chen, F. C., Koopmans, G., Wiseman, R. L., Day, L. A., & Swinney, H. L. (1980) *Biochemistry 19*, 1373–1376.

Cowman, M. K., & Fasman, G. D. (1978) *Proc. Natl. Acad. Sci. U.S.A. 75*, 4759–4763.

Crothers, D. M., Dattagupta, N., Hogan, M., Klevan, L., & Lee, K. S. (1978) *Biochemistry 17*, 4525–4533.

Davies, H. G. (1968) *J. Cell Sci. 3*, 129–150.

de Murica, G., Das, G. C., Erard, M., & Daune, M. (1978) *Nucleic Acids Res. 5*, 523–535.

Ding, D. W., Rill, R., & Van Holde, K. E. (1972) *Biopolymers 11*, 2109–2124.

Eisenberg, H., & Tomkins, G. M. (1968) *J. Mol. Biol. 31*, 37–49.

Everid, A. C., Small, J. V., & Davies, H. G. (1970) *J. Cell Sci. 7*, 35–48.

Finch, J. T., & Klug, A. (1976) *Proc. Natl. Acad. Sci. U.S.A. 73*, 1897–1901.

Finch, J. T., Lutter, L. C., Rhodes, D., Brown, R. S., Rushton, B., Levitt, M., & Klug, A. (1977) *Nature (London) 269*, 29–36.

Fulmer, A., & Fasman, G. (1979) *Biochemistry 18*, 659–668.
Griffith, J., & Christiansen, G. (1978) *Annu. Rev. Biophys. Bioeng. 7*, 19–35.
Hogan, M., Dattagupta, N., & Crothers, D. M. (1978) *Proc. Natl. Acad. Sci. U.S.A. 75*, 195–199.
Houssier, C., & Fredericq, E. (1966) *Biochim. Biophys. Acta 120*, 113–130.
Houssier, C., Bontemps, J., Emonds-Alt, X., & Fredericq, E. (1977) *Ann. N.Y. Acad. Sci. 303*, 170–189.
Lee, K. S. (1980) Ph.D. Thesis, Yale University.
Marion, C., & Roux, B. (1978) *Nucleic Acids Res. 5*, 4431–4449.
McDonnell, M. W., Simon, M. N., & Studier, F. W. (1977) *J. Mol. Biol. 110*, 119–146.
Newman, J., Swinney, H., & Day, L. A. (1977) *J. Mol. Biol. 116*, 593–606.
O'Konski, C. T., Yoshioka, K., & Orttung, W. H. (1959) *J. Phys. Chem. 63*, 1558–1565.
Olins, A. L. (1977) *Biophys. J. 17*, 115a.
Olins, A. L. (1978) *Cold Spring Harbor Symp. Quant. Biol. 42*, 325–329.
Olins, A. L., & Olins, D. E. (1979) *J. Cell Biol. 81*, 260–265.
Olins, A. L., Carlson, R. D., Wright, E. B., & Olins, D. E. (1976) *Nucleic Acids Res. 3*, 3271–3291.
Renz, M., Nehls, P., & Hozier, J. (1977) *Proc. Natl. Acad. Sci. U.S.A. 74*, 1879–1883.
Renz, M., Nehls, P., & Hozier, J. (1978) *Cold Spring Harbor Symp. Quant. Biol. 42*, 245–252.
Rill, R., & Van Holde, K. E. (1974) *J. Mol. Biol. 83*, 459–471.
Ris, H. (1973) *Ciba Found. Symp. 28*, 7–22.
Steinmetz, M., Streeck, R. Z., & Zachau, H. G. (1978) *Eur. J. Biochem. 83*, 615–628.
Suan, P., Bradbury, E. M., & Baldwin, J. P. (1979) *Eur. J. Biochem. 97*, 593–602.
Thoma, F., Koller, Th., & Klug, A. (1979) *J. Cell Biol. 83*, 403–427.
Tinoco, I. (1955) *J. Am. Chem. Soc. 77*, 4486–4489.
Tirado, M. M., & Garcia de la Torre, J. (1979) *J. Chem. Phys. 71*, 2581–2587.
Weber, K., & Osborn, M. (1969) *J. Biol. Chem. 244*, 4406–4412.
Worcel, A., & Benyajati, C. (1977) *Cell 12*, 83–100.
Wu, H. M., Dattagupta, N., Hogan, M., & Crothers, D. M. (1979) *Biochemistry 18*, 3960–3965.
Zirkin, B. R., & Wolfe, S. L. (1972) *J. Ultrastruct. Res. 39*, 496–508.

Phosphorylation States of Different Histone 1 Subtypes and Their Relationship to Chromatin Functions during the HeLa S-3 Cell Cycle†

Kozo Ajiro,‡ Thaddeus W. Borun, and Leonard H. Cohen*

ABSTRACT: The histone 1 (H1) fraction of HeLa S-3 cells contains two principal subtypes, H1A (M_r ~21 000) and H1B (M_r ~22 000). In G_1 cells, the H1 molecules are distributed among several phosphorylation states, most H1A molecules containing 0 or 1 phosphate groups and most H1B molecules containing 0, 1, 2, or 3 phosphate groups. Both subtypes undergo a general increase in phosphorylation levels of ~1 P/mol during the S phase and a further increase of 3–4 P/mol during mitosis. These two increases affect most of the H1 molecules and thus reflect phosphorylations occurring widely throughout the chromatin, presumably in association with replication and mitotic chromosome condensation. During all these periods, multiple phosphorylation levels of H1 molecules persist, as does the phosphorylation differential between H1A and H1B. Thus, there appear to be phosphorylation states that only some of the H1 molecules occupy, a fact that may be related to the conformational diversity in interphase and mitotic chromatin. The existence of differences between H1A and H1B phosphorylation states throughout the cell cycle, and within a single cell type, is in accord with the hypothesis that the H1 subtypes are functionally distinct, such that subtype-specific phosphorylations contribute to the control of chromatin organization.

The eukaryotic cell is thought to be able to exert control over fine details of the organization of its chromatin (Comings, 1972; Sedat & Manuelides, 1978). This degree of control undoubtedly reflects a number of functional needs: during interphase, active genes must be exempt from the high degree of compaction required to keep the large eukaryotic genome within reasonable physical bounds; there must be a precise schedule of unpackaging of genomic segments for purposes of replication; and after replication has been completed, the chromatin must be folded reproducibly into the variety of ordered structures of the mitotic chromosomes. A major element in the control of chromatin organization is histone 1 (H1),[1] which plays a role in the higher order coiling of the elemental chromatin fiber (Mirsky et al., 1968; Bradbury et al., 1973; Worcel, 1978; Cole et al., 1978; Gaubatz et al., 1978; Renz et al., 1978; Oudet et al., 1978).

† From The Wistar Institute of Anatomy and Biology, Philadelphia, Pennsylvania 19104 (K.A. and T.W.B.), and The Institute for Cancer Research, Fox Chase Cancer Center, Philadelphia, Pennsylvania 19111 (L.H.C.). *Received January 3, 1979.* This investigation was supported by U.S. Public Health Service Research Grants CA-11463, CA-12544, CA-21069, CA-06927, and CA-17856 from the National Cancer Institute and GM-24019 from the National Institute of General Medical Sciences, and an appropriation from the Commonwealth of Pennsylvania. T.W.B. was a recipient of Research Career Development Award CA-00088 from the National Cancer Institute. We dedicate this and the subsequent paper to his memory.

‡ Present address: Aichi Cancer Center, Research Institute, Laboratory of Cell Biology, Chikusa-ku, Nagoya 464, Japan.

[1] Abbreviations used: H1, histone 1; PCA, perchloric acid; Cl_3CCO-OH, trichloroacetic acid; MeOH, methanol; HOAc, acetic acid; GdmCl, guanidinium chloride; CHO, Chinese hamster ovary.

0006-2960/81/0420-1445$01.25/0